Kawahara et al., J Textile Sci Eng 2015, 5:6
DOI: 10.4172/2165-8064.1000219

Journal of Textile Science & Engineering

Research Article Open Access

Direct Carbonization of High-performance Aromatic Polymers and the Production of Activated Carbon Fibers

Yutaka Kawahara[1,2]*, Shunsuke Otoyama[1], Kazuyoshi Yamamoto[3], Hiroyuki Wakizaka[4], Yutaka Shinahara[5], Hideki Hoshiro[6], Noboru Ishibashi[3] and Norio Iwashita[7]

[1]*Division of Environmental Engineering Science, Gunma University, Tenjin-cho, Kiryu 376-8515, Japan*

[2]*The Center for Fiber and Textile Science, Kyoto Institute of Technology, Matsugasaki, Sakyo-ku, Kyoto 606-8585, Japan*

[3]*Research Lab., Carbo-tec. Co. Ltd., 305, Creation Core Kyoto Mikuruma, Kajii, Kamigyo-ku, Kyoto 602-0841, Japan*

[4]*North Eastern Industrial Research Center of Shiga Prefecture, 27-39, Mitsuyamotomachi, Nagahama, Shiga 526-0024, Japan*

[5]*Nippon Felt Co. Ltd., Saitama Mill, 88, Haramamuro, Kounosu, Saitama 365-0043, Japan*

[6]*Kuraray Co. Ltd., North Umeda Hankyu Building Office Tower, 8-1, Kakudacho, Kita-ku, Osaka 530-8611, Japan*

[7]*National Institute of Advanced Industrial Science and Technology, 16-1, Onokawa, Tsukuba, Ibaragi 305-8569, Japan*

Abstract

For expanding the utilization of several high-performance aromatic polymeric fibers, e.g., poly *p*-phenylene benzobisoxazole (PBO, Zylon®), poly *p*-phenylene terephthalamide (PTA, Kevlar 29®), and polyarylate (PA, Vectran®), direct carbonizing and graphitizing behaviors have been investigated. The PBO-based carbon fiber showed a typical radial texture on its fracture surface, and the graphitization degree (P1) reached 0.35 and crystallite sizes of Lc(002), La(110) after graphitization exceeded 30 nm. On the other hand, the P1 indices of the graphitized carbon fibers from PTA and PA were no more than 0.15. However, a low P1 value is preferable for the production of activated carbon fibers (ACF). In addition, on the surface of the PA-based carbon fibers produced at 900°C, some fine mesh-like morphologies were observed indicating the formation of a porous carbon structure. In contrast, for the PTA-based carbon fibers the development of radial texture could be seen only partially on the fracture surface, and porous morphologies were not recognizable. It was confirmed that the direct carbonization was enough to convert PA fibers into ACF. The BET surface area of the PA-based carbon fibers increased up to 900~1,000 m^2/g after the direct carbonization at 900 °C, and exceeded 1,000 m^2/g easily when activated.

Keywords: Activated carbon fibers; Aromatic polymers; Carbonization; Graphitization; Poly p-phenylene benzobisoxazole; Poly p-phenylene terephthalamide; Polyarylate

Introduction

Nowadays, polyacrylonitrile (PAN) and pitch, a heavy fraction of petroleum, are the two major starting materials for producing high-performance carbon fibers. For most high-volume applications, however, it is necessary to consider their production costs due to the lengthy, multistep process for the conversion of starting precursor fibers into high-performance carbon fibers. During the processing, the precursor fibers require oxidative stabilization prior to carbonization heat-treatment. This oxidative stabilization step is slow and affects the final mechanical properties of the carbon fibers. Therefore, direct carbonization has been tried using high-performance aromatic polymeric fibers, e.g., poly *p*-phenylene benzobisoxazole (PBO) [1-5], and Kevlar [6]. Especially, PBO-based carbon fibers obtained by the direct carbonization have once attracted remarkable attention. However, it was difficult to produce high-performance carbon fibers because the flaws present in the precursor fibers persisted throughout the carbonization and caused tensile failures of the carbonized fibers. Moreover, the release of nitrogen over 1,400°C affected the tensile strengths of the carbonized fibers [2,3]. Therefore, the graphitizing properties of these high-performance aromatic polymeric fibers have not been fully studied so far although they may be useful for the preparation of not only the carbon fibers but also activated carbon fibers (ACF), electrodes of secondary batteries, etc. For the production of these carbon goods from aromatic polymers, simple direct carbonization process is attractive to save the production cost. For this purpose, it is necessary to clarify their carbonizing and graphitizing behaviors.

At present, non-woven fabrics made of the high-performance aromatic polymeric fibers are often used as heat resistant or thermal insulating cushions, e.g., the roller covers in the rolling process of aluminum rod production. Therefore, for these purposes, also, it is important to understand the carbonization behavior of these super fibers. Moreover, in the production process of non-woven fabrics, the generation of raw edges that are severed and wasted is inevitable, which increases the production costs. However, these waste ends made of high-performance aromatic polymeric fibers may have a potential for the production of carbon fibers via the direct carbonization. Although it is not easy to produce carbon fibers with excellent tensile properties, carbon fibers with specific properties, e.g., heat resistance, absorption properties, electrical conductivity [2], chemical resistance, could be producible.

In this paper, direct carbonization experiments were attempted using high-performance aromatic polymeric fibers, i.e., PBO (Zylon®), poly *p*-phenylene terephthalamide (PTA, Kevlar 29®), and polyarylate

***Corresponding author:** Yutaka Kawahara, Professor, Division of Environmental Engineering Science, Gunma University, 1-5-1, Tenjin-cho, Kiryu 376-8515, Japan, Tel/Fax: 81-277-30-1491; E-mail: kawahara@gunma-u.ac.jp

Received November 02, 2015; **Accepted** November 10, 2015; **Published** November 20, 2015

Citation: Kawahara Y, Otoyama S, Yamamoto K, Wakizaka H, Shinahara Y, et al. (2015) Direct Carbonization of High-performance Aromatic Polymers and the Production of Activated Carbon Fibers. J Textile Sci Eng 5: 219. doi:10.4172/2165-8064.1000219

(PA, Vectran®), and then their graphitizing properties were compared firstly. The PBO-based carbon fiber showed a larger graphitization degree (P1) and crystallite sizes. In contrast, the P1 indices of the carbon fibers from PTA and PA were fairly small. However, it was confirmed that carbon fibers with BET surface areas of ~1,000 m^2/g could be produced via the direct carbonization from PA fibers.

Materials and Methods

Materials

The PBO and PTA fibers were raw edges of non-woven fabrics supplied by Nippon Felt Co., Ltd. (Saitama, Japan), and the PA fibers were from Kuraray Co., Ltd. (Osaka, Japan). The PA fibers used were produced from the melt spinning of a co-polymer of 1,4 hydroxybenzoate and 2,6 hydroxynaphthanoate in the monomer ratio of 73/27, respectively, followed by the thermosetting treatment to elevate the melting temperature of the fibers.

Carbonization and activation at the laboratory-scale

The starting fibers of 4 to 5 g, released from contact with each other, were heated at a rate of 10°C/min, and then kept at 900°C for 60 min using an electric furnace having a uniform temperature zone of about 60 mm in length under nitrogen gas flowing at 1 L/min followed by cooling to room temperature.

To activate the carbon fibers, a rotary kiln (internal volume of ca. 0.75 L) was used. First, ca. 2 g of the fibers was heated to 900°C at a heating rate of 10°C/min under nitrogen gas flowing at 0.6 L/min, and then kept at 900°C for 10 min for activation while water vapor was added instead of nitrogen gas.

Heat-treatment at 3,000°C

Carbonized samples were heated almost linearly from room temperature to 3,000°C in 140 min, and were kept at 3,000°C for 30 min, and then left to cool to room temperature using an electric furnace (SCC-U-120/203/135, Kurata Giken Co., Konan, Shiga, Japan); argon gas was flowing throughout.

Thermogravimetric analysis/differential thermal analysis (TG/DTA) measurement

TG/DTA measurements were performed using an analyzer (WS-002, Bruker AXS K.K., Yokohama, Japan) on 10 mg of sample at a heating rate of 20°C/min up to 1,000°C under nitrogen gas flowing at 50 mL/min.

X-ray diffraction

Wide-angle X-ray diffraction (WAXD) was performed on isotropic samples which were obtained by grinding and mixing the carbonized fibers with high-purity silicon powder as the inner standard. The X-ray source was CuK_α radiation.

The degree of graphitization (P1), defined as the probability for adjacent hexagonal carbon layers to have the positional correlation in graphite, was determined from the Fourier coefficients of both the 101 and 112 WAXD peak profiles measured using step-scanning with a step of 0.01 °C and an accumulation time of 30 s [7,8]. The average interlayer spacing was calculated using the Bragg's equation from the peak diffraction angles of the carbons determined by referring to the diffraction of the silicon standard. The average interlayer spacings determined from the 002, 004, and 006 diffractions were denoted as d_{002} (002), d_{002}(004), and d_{002}(006), respectively. The crystallite sizes parallel and perpendicular to the *c*-axis (Lc and La) were calculated from the full-width at half-maximum for the diffraction peaks of the carbons, which were corrected for the instrumental peak broadening by referring to the diffractions of the silicon standard. The size parameters determined from the 002, 004, 006, and 110 diffractions using the Scherrer's equation were denoted as Lc(002), Lc(004), Lc(006), and La(110), respectively. The standard deviation of the distribution in the interlayer spacing (σ_c) and the true crystallite size parallel to the *c*-axis (L_o) were determined using the Hosemann's equation [9].

$$[1/\mathrm{Lc}(00l)]^2 = [1/L_o]^2 + \pi^4\sigma_c^4 l^4/[16 d_{002}(004)^6] \quad (1)$$

where l is the order of the diffraction.

Adsorption characterization

The nitrogen gas adsorption capacity was determined using an adsorption measurement instrument (BELSORP-18plus, BEL Inc. Jpn, Toyonaka, Japan). The pore surface area (S) was determined using the Brunauer–Emmett–Teller (BET) plot [10]. The pore volume (V) was determined from the amount of nitrogen adsorbed at a relative pressure of 0.99. The mean pore diameter (D) was calculated as $D = 4V/S$ by assuming that the pores were uniform non-intersecting cylindrical capillaries.

Results and Discussion

Carbonization behavior

TG and DTA curves for the PBO fibers are shown in Figure 1. It is seen from the TG curve that the thermal decomposition of PBO fibers occurred in two steps, i.e., over 420°C and 660°C, similarly as in previous data [1,2]. The carbon yield at 1,000°C was ca. 60%. It has been reported that heat-treatment at 600°C is effective to improve the level of crystallinity in core regions of PBO fibers [1]. However, an exothermic peak corresponding to the crystallization of PBO molecules was not observed. On the other hand, it has been demonstrated that PBO fibers begin to pass from the ordered initial state to an amorphous state when heated over approximately 600°C [2], and the carbonization of PBO fibers can be modeled as a free-radical polymerization [4]. Thus, the sudden decrease in the TG curve over 660°C probably means that free-radical polymerization was occurring accompanying the thermal cracking of the PBO backbones. Thereby, the DTA exothermic peak at 678°C can be attributed to this thermal cracking and the peak at 750°C to the polycondensation to form carbon structure.

The surface of the PBO-based carbon fibers produced at 900C is shown in Figure 2a. The striations along the fiber axis are due to the development of a radial structure. No periodic banded structure along

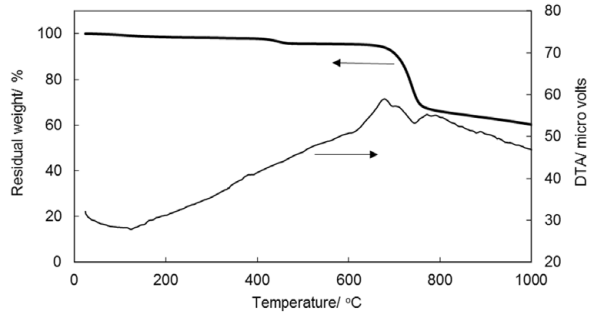

Figure 1: TG and DTA curves for PBO fibers: bold, TG; fine, DTA.

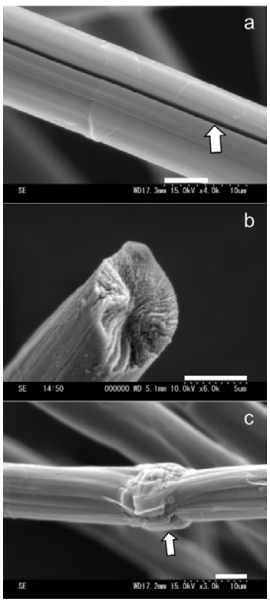

Figure 2: SEM images for PBO-based carbon fibers: (a) fissure running along the fiber axis (when carbonized at 900°C); (b) and (c), radial texture in the fracture surface and a swelling generated by the nitrogen puffing, respectively (when carbonized at 3,000°C). The scale bars are 5 μm.

the fiber axis could be recognized. These features coincide with the previous work on PBO-based carbon fibers [1]. It is well known that PBO-based carbon fibers will show a fracture surface having carbon layers stacked radially from the center [2]. In addition, most of the PBO-based carbon fibers exhibit so-called "open wedge texture" when heated over 900°C [5]. Therefore the fissure running along the fiber axis (refer to the arrow in Figure 2a) seems to be brought about by the development of the radial structure. The radial texture in the fracture surface became obvious with elevating the heat-treatment temperature. The fracture surface of PBO-based carbon fiber produced at 3,000°C showed a typical radial pattern (see Figure 2b). Moreover, another peculiar morphology, like a swelling, interfering with the running of striations (refer to the arrow in Figure 2c) could be observed at intervals on the surface of PBO-based carbon fibers produced at 3000°C. Such swelling is probably due to the nitrogen puffing or linear expansion of the carbon layers that occurs under released conditions over 1,400°C [2].

TG and DTA curves for the PTA fibers are shown in Figure 3. The TG curve obtained suggests that the thermal decomposition of PTA fibers proceeded in three steps, i.e., over 400, 540, and 600°C. The carbon yield at 1,000°C was 28.9% and still decreasing. In the case of Kevlar 49 fibers, however, the abrupt one-step weight decrease was observed between 450°C and 550°C [6]. On the other hand, the DTA curve corresponding to the temperature range of the 2nd step in the TG curve showed an exothermic shoulder and a peak at 570°C, and 610°C, respectively, while there was no such remarkable DTA shoulder or peak for the other steps. It is seen that the polycondensation reactions abruptly occurred and was concentrated in the 2nd step for the PTA fibers, i.e., 540～630°C, a little higher than the thermal decomposition temperature range of Kevlar 49 fibers.

An SEM image of the broken end of a PTA-based carbon fibers produced at 3,000°C is shown in Figure 4a. A clear banded structure on the fracture surface with a periodicity of ~500 nm could be recognized along the fiber axis, similarly as in a previous work on Kevlar 49-based carbon fibers [6]. In the case of the pristine Kevlar 49 fibers, the higher-order structure was described as radially arranged pleated sheets alternating the crystallite orientation periodically in a similar length of ~500 nm along the fiber axis [11]. This inherent arrangement of crystallites will affect the stacking of carbon layers when carbonized. Therefore, the PTA-based carbon fibers showed periodic bands on the fracture surface. In the fracture surface of PTA-based carbon fibers heat-treated at 3,000°C (Figure 4b), the development of radial structure could be partially recognized. Overall, however, the texture was not so marked as expected from the higher-order structural model of Kevlar 49 fibers described above.

TG and DTA curves for the PA fibers are shown in Figure 5. From the TG curve it seems that the thermal decomposition of PA fibers proceeded in one step, abruptly, between 490 and 550°C, and almost ceased at 1,000°C. The carbon yield at 1,000°C was 33.4%. However, the DTA peaks and shoulders over 540°C indicate that the polycondensation reactions proceeded in several steps competitively and interactively, then only a monotonic decrease in the TG curve was seemingly observed.

The PA fibers were produced from melt spinning followed by a thermosetting treatment which could enhance the thermal stability, accompanying by crystal modification from psudo-hexagonal of as-spun fibers to orthorhombic [12], and increasing the average molecular

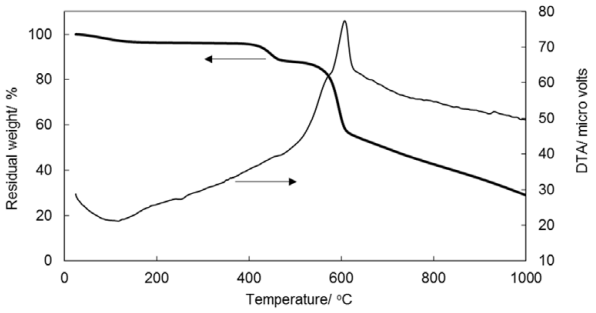

Figure 3: TG and DTA curves for PTA fibers: bold, TG; fine, DTA.

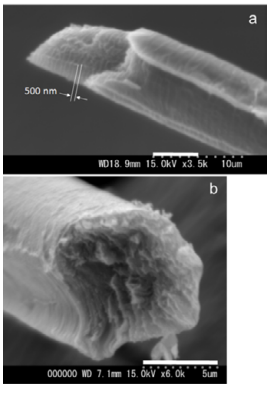

Figure 4: SEM images for PTA-based carbon fibers produced at 3,000°C: (a) broken end, (b) fracture surface. The scale bars are 5 μm.

weight through the solid-state polymerization (SSP) that could elevate the melting temperature of the heat-treated fibers [13]. The small endotherm at ~318°C (refer to an arrow in Figure 5) can therefore be attributed to the melting of crystallites in the heat-treated PA fibers. However, the increase of viscosity in the amorphous regions induced by SSP was large enough to prevent the fibers from fusing.

The surface of the PA-based carbon fibers produced at 900°C is shown in Figure 6a. The formation of bands on the exterior surface was much more obvious compared with the PTA-based carbon fibers. This is probably related to the fact that the pristine fibers contain the banded structure generated by the orientation of crystallites of liquid crystalline PA [14]. Moreover some fine mesh-like morphologies could also be observed (refer to an arrow in Figure 6a). Such morphologies will be advantageous to increase the BET surface area if the PA-based carbon fibers are applied to the production of ACF. The surface of PA-based carbon fibers produced at 3,000°C is shown in Figure 6b. The banded structure on the surface of fiber was not so marked and the fracture surface texture became featureless. This is probably related to the low graphitization degree, P1, of PA (Table 1). The particles deposited on the surface of the fiber are probably due to the chemical vapor deposition reactions with decomposition gases.

For the preparation of the roller cushions in the rolling process of aluminum rod production, PBO fiber is preferable due to its high heat resistance to 600°C. However, PBO fiber has been shown here to not be appropriate for the production of carbon fibers free from fissures or swellings. On the other hand, the porous morphologies observed on PA-based carbon fibers suggest the potential for the development of ACF.

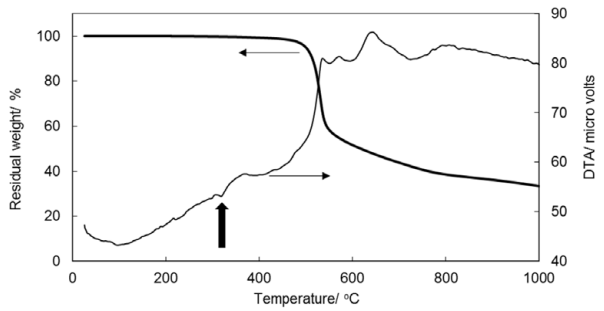

Figure 5: TG and DTA curves for PA fibers: bold, TG; fine, DTA.

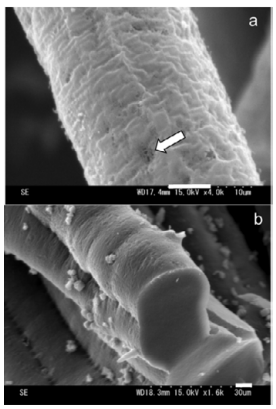

Figure 6: SEM images for PA-based carbon fibers produced at (a) 900°C, (b) 3,000°C. The scale bars are 5 μm.

Sample	PBO	Kevlar29	Polyarylate	Cellulose [16]
P1	0.35	0.15	0.13	0.13
***d*002(002), nm**	0.3366	0.3398	0.3404	0.3393
***d*002(004), nm**	0.3360	0.3397	0.3390	0.3388
***d*002(006), nm**	0.3361	–	–	–
Lc(002), nm	30	11	5	14
Lc(004), nm	20	7	4	8
Lc(006), nm	16	–	–	–
La(110), nm	39	6	3	11
σ_c, nm	0.006	0.011	0.012	0.010
L_0, nm	31	7	5	15

Table 1: Crystallite structure of the carbon fibers produced at 3,000°C.

Graphitizing properties of aromatic polymers

In general, the graphitizing property of the starting material will determine its industrial usability as carbon products. That is, the composition of the starting material and the chemical structure of each component affect the carbon structure and its yield. Carbon is usually classified into graphitizing and non-graphitizing types [15]. The graphitizing property can be estimated by measuring the graphitization degree, P1. In fact, carbonaceous materials with large P1 tend to be transformed into a charcoal with graphite-like structure. In the case of pure graphite, P1 equals one. Such densely packed structure, however, is not suitable for the production of ACF because the diffusion of activation gases, such as water vapor or CO_2, into the carbonaceous materials would be inhibited and an ACF displaying only limited adsorption-capacity forms. Therefore, the graphitization degree should be controlled within a certain range, e.g., P1~0.1, for ACF applications. Another important property determining the applicability to ACF is a capability of organizing a porous carbon structure. Therefore, the PA fibers with these two important properties were more preferable for the starting material to produce ACF compared with the PTA yielding non-graphitizing solid carbon without a porous carbon structure.

The graphitizing heat-treatment on the carbon fibers produced at 900°C was conducted at 3,000°C, and the P1 indices were estimated using WAXD. The P1 index, 002 spacings based on the various orders and the corresponding crystallite sizes are listed in Table 1. The 006 diffraction peak could not be observed except for PBO due to disordering in the stacking of adjacent hexagonal carbon layers. Therefore, the standard deviation of the distribution in the interlayer spacing (σ_c) was enlarged for the PTA, PA, and cellulose [16]. The P1 value became the largest for the PBO-based carbon fibers that showed the typical radial texture on their fracture surface. On the other hand, the PTA and PA, with smaller P1 indices, should be categorized into non-graphitizing starting materials.

From the viewpoint of graphitizing properties, the PBO fibers, with higher P1 index, were better converted into short carbon fibers after graphitization and could be used as fillers to give functionalities to composite materials, such as electrical conductivity, rigidity, etc. As for the PTA fibers, the fibers were non-graphitizable and could be used as general-performance carbon fibers after appropriate carbonization by controlling the heating rate, the heat-treatment temperature etc.

Production of ACF by direct carbonization of PA fibers

Cellulosic materials that have been classified as non-graphitizing

Carbonization at 900°C (N_2, 1 h)	
Yield, %	39.3
BET area, m^2/g	927
BET volume, mL/g	0.37
Mean pore diameter, nm	1.61
Activation at 900°C (H_2O, 10 min)	
Yield, %	58.8
BET area, m^2/g	1,339
BET volume, mL/g	0.56
Mean pore diameter, nm	1.67

Table 2: Yields and surface characteristics of polyarylate-based carbon fibers.

carbon are often used as starting materials in the production of ACF destined for drinking water and/or wastewater control systems. Non-graphitizing carbons are highly attractive for ACF production to ensure an effective reaction with activation gases, leading to porous structures with large adsorption capacity. Activated carbon materials with BET surface area exceeding 1,000 m^2/g can easily be produced from woody biomass [17,18]. When the graphitizing property and crystal parameters of PA-based carbon fibers were compared with those of a cellulose-based one here, cellulosic materials extracted from reed grass (Table 1) [16], they ranged within similar values. In addition, the PA fibers showed porous morphologies when carbonized (Figure 6a), which would be advantageous for the production of ACF although to our knowledge, never tried so far.

Yields and surface characteristics of the PA-based carbon fibers are listed in Table 2. The yield of ACF was defined as the relative mass of ACF against the mass of carbon fibers before activation. The BET surface area reached 1,339 m^2/g when activated to the weight-loss of ca. 40%. However, it is seen that merely carbonization was enough to gain a BET surface area to 900~1,000 m^2/g. Moreover, the mean pore diameter was almost comparable to woody biomass-based ACs of 1.8~2.1 nm [16,18], implying that the direct carbonization is enough to convert PA fibers into ACF destined for drinking water and/or wastewater control systems.

Conclusion

Carbonizing and graphitizing behaviors for three high-performance aromatic polymers have been investigated. The PBO-based carbon fiber showed the typical radial texture on its fracture surface, and the P1 index reached 0.35 and crystallite sizes of Lc(002), La(110) after graphitization exceeded 30 nm. On the other hand, the P1 indices of the graphitized carbon fibers from PTA and PA were no more than 0.15. Therefore PTA and PA could be categorized as yielding non-graphitizing carbon. However, a low P1 value is preferable for the production of ACF. A starting material with a high P1 value tends to be transformed into a carbon with densely packed structure, which is not suitable for the production of ACF because the diffusion of activation gases, such as water vapor or CO_2, into the carbonaceous materials tends to be inhibited and an ACF displaying only limited adsorption-capacity forms. Moreover, a starting material should have a capability of organizing a porous carbon structure. On the surface of PA-based carbon fibers produced at 900°C, some fine mesh-like morphologies were observed, which suggests that carbon fibers with porous structure could be produced from the PA fibers. From this structural viewpoint, the PA fibers are more preferable to the PTA. The BET surface area was measured on the PA-based carbon fibers and it was found that the value increased up to 900~1,000 m^2/g after carbonization at 900°C, and exceeded 1,000 m^2/g easily when activated. It can be concluded, at least, that direct carbonization is enough to convert PA fibers into ACF.

References

1. Young RJ, Day RJ, Zakikhani M (1990) The structure and deformation behavior of poly(p-phenylene benzobisoxazole) fibers. J Mater Sci 25: 127-136.
2. Newell JA, Rogers DK, Edie DD, Fain CC (1994) Direct carbonization of PBO fiber. Carbon 32: 651-658.
3. Newell JA, Edie DD (1996) Factors limiting the tensile strength of PBO-based carbon fibers. Carbon 34: 551-560.
4. Newell JA, Edie DD, Fuller ELJr (1996) Kinetics of carbonization and graphitization of PBO fiiber. J Appl Polym Sci 60: 825-832.
5. Kaburagi Y, Yokoi K, Yoshida A, Hishiyama Y (2005) Highly graphitized carbon fiber prepared from poly(p-phenylene-benzo-bis-oxazole) fiber. Tanso 217: 111-114.
6. Tomizuka I, Isoda Y, Amamiya Y (1981) Carbon fibre from a high-modulus polyamide fibre (Kevlar). Tanso 106: 93-101.
7. Houska CR, Warren BE (1954) X-Ray study of the graphitization of carbon black. J Appl Phys 25: 1503-1509.
8. Noda T, Iwatsuki M, Inagaki M (1966) Changes of probabilities P1, $P_{ABA, PABC}$ with heat treatment of carbons. Tanso 47: 14-23.
9. Shioya M, Takaku A (1989) Characterization of the structure of carbon fibers by wide-angle and small-angle X-ray scatterings. Tanso 139: 189-198.
10. Adamson AW (1991) Physical chemistry of surfaces. John Wiley and Sons, New York, USA.
11. Dobb MG, Johnson DJ, Saville BP (1977) Supramolecular structure of a high-modulus polyaromatic fiber (Kevlar 49). J Polym Sci, Polym. Phys Ed 15: 2201-2211.
12. Cohen EK, Marom G, Weinberg A, Wachtel E, Migliaresi C, et al. (2007) Microstructure and nematic transition in thermotropic liquid crystalline fibers and their single polymer composites. Polym Adv Technol 18: 771-779.
13. Yamamoto Y, Nakagawa J (2009) The structure and properties of high-modulus, high-tenacity Vectran™ fibers.
14. Taylor JE, Romo-Uribe A, Libera MR (2003) Molecular orientation gradients in thermotropic liquid crystalline fiber. Polym Adv Technol 14: 595-600.
15. Oberlin A, Oberlin M (1983) Graphitizability of carbonaceous materials as studied by TEM and X-ray diffraction. J Microsc 132: 353-363.
16. Kawahara Y, Yamamoto K, Wakisaka H, Izutsu K, Shioya M, et al. (2009) Carbonaceous adsorbents produced from coffee lees. J Mater Sci 44: 1137-1139.
17. Ishibashi N, Yamamoto K, Wakisaka H, Kawahara Y (2014) Influence of the hydrothermal pre-treatments on the adsorption characteristics of activated carbons from woods. J Polym and the Environ 22: 267-271.
18. Kawahara Y, Izumoto M, Nishikawa G, Wakisaka H, Iwashita N, et al. (2006) Carbonization behavior of reed grass and production of activated carbon. Sen'i Gakkaishi 62: 242-244.